

1    **Isolating the Impacts of Land Use and Climate Change on Streamflow**

2    **Ila Chawla<sup>1</sup> and P.P. Mujumdar<sup>1,2</sup>**

3    [1]{Department of Civil Engineering, Indian Institute of Science, Bangalore, India}

4    [2]{Divecha Center for Climate Change, Indian Institute of Science, Bangalore, India}

5    Correspondence to: P. P. Mujumdar ([pradeep@civil.iisc.ernet.in](mailto:pradeep@civil.iisc.ernet.in))

6

## Isolating the Impacts of Land Use and Climate Change on Streamflow

Ila Chawla<sup>1</sup> and P.P. Mujumdar<sup>1, 2</sup>

[1]{Department of Civil Engineering, Indian Institute of Science, Bangalore, India}

[2]{Divecha Center for Climate Change, Indian Institute of Science, Bangalore, India}

Correspondence to: P. P. Mujumdar ([pradeep@civil.iisc.ernet.in](mailto:pradeep@civil.iisc.ernet.in))

### Abstract

Quantifying the isolated and integrated impacts of land use and climate change on streamflow is challenging as well as crucial to optimally manage water resources in the river basin. This paper presents a simple hydrologic modelling based approach to segregate the impacts of land use and climate change on streamflow of a river basin. The Upper Ganga Basin in India is selected as the case study to carry out the analysis. Streamflow in the river basin is modelled using a calibrated Variable Infiltration Capacity hydrologic model. The approach involves development of three scenarios to understand the influence of land use and climate on streamflow. The first scenario assesses the sensitivity of streamflow to land use changes under invariant climate. The second scenario determines the change in streamflow due to change in climate assuming constant land use. The third scenario estimates the combined effect of changing land use and climate over streamflow of the basin. Based on the results obtained from the three scenarios, quantification of isolated impacts of land use and climate change on streamflow is addressed. Future projections of climate are obtained from dynamically downscaled simulations of six general circulation models (GCMs) available from the Coordinated Regional Downscaling Experiment (CORDEX) project. Uncertainties associated with the GCMs and emission scenarios are quantified in the analysis. Results for the case study indicate that streamflow is highly sensitive to change in urban area and moderately sensitive to change in crop land area. However, variations in streamflow generally reproduce the variations in precipitation. Combined effect of land use and climate on streamflow is observed to be more pronounced compared to their individual impacts in the basin. It is observed from the isolated effects of land use and climate change that climate has a more dominant impact on streamflow in the region. The approach proposed in this paper is applicable to any river basin to isolate the impacts of land use change and climate change on the streamflow.

## 1 Introduction

Land use (LU) and climate are the drivers of hydrologic processes in a river basin (Vörösmarty et al., 2000; Nijssen et al., 2001; Oki and Kanae, 2006; Wada et al., 2011). Change in LU is observed to influence the hydrological cycle and the availability of water resources by altering interception, infiltration rate, albedo and evapotranspiration (ET) (Rose and Peters, 2001; Scanlon et al., 2007; Rientjes et al., 2011). Climate in contrast affects the basic components of hydrologic cycle such as precipitation, soil moisture, evaporation and atmospheric water content (Gleick, 1986; Wang et al., 2008). Therefore, understanding the hydrologic response of a river basin to changes in LU and climate forms a critical step towards water resources planning and management (Vörösmarty et al., 2000). Moreover, with increase in scarcity of water resources, hydrologic impacts of LU and climate change has drawn significant attention from the hydrologic community (Scanlon et al., 2007). In this regard, several studies have been carried out that focus on understanding exclusive impacts of either of the two drivers (Hamlet and Lettenmaier, 1999; Christensen and Lettenmaier, 2007; Beyene et al. 2010; Wagner et al., 2013; Islam et al., 2014). However, optimum management of water resources in a river basin needs an in depth understanding of the isolated and integrated effects of LU and climate on streamflow. Due to complex response of streamflow to combined effects of LU and climate change (Fu et al., 2007; Guo et al., 2008), very few studies have been carried out on this aspect (Mango et al., 2011; Guo et al., 2008; Cuo et al., 2013; Wang et al., 2013). Segregating the individual contribution of LU and climate to streamflow has recently become the focus of scientific work (Wang and Hejazi, 2011; Wang et al., 2013; Renner et al., 2012; Renner et al., 2014).

Methods used to assess the impacts of LU and climate on streamflow can be broadly classified into four categories (i) experimental paired catchment approach; (ii) statistical techniques such as Mann-Kendall test; (iii) empirical or conceptual models and (iv) distributed physically-based hydrologic models. Among these techniques, the paired catchment approach is most difficult but often considered as the best approach for smaller catchments. However, applicability of paired catchment approach over large catchments may not be possible (Lørup et al., 1998) since it requires years of continuous monitoring to gather sufficient data for the analysis. Statistical trend detection tests have been proved to be very useful in qualitatively determining the presence of significant trend in the time series along with direction and rate of change (Zhang et al., 2008; Li

et al., 2009). But these techniques cannot be used for quantifying the change and attributing it to a particular cause due to lack of physical mechanism (Li et al., 2009). Empirical or conceptual models are simple hydrologic models that require only a few parameters to simulate a catchment. However, a major drawback with these models is that the parameters may not be directly related to the physical conditions of the catchment and thus may lack the ability to correctly represent a catchment. Therefore, one is left with the option of using distributed physically based hydrologic models, which are by far the most appealing tools to carry out impact assessment studies (Ott and Uhlenbrook, 2004; Mango et al., 2011; Wang et al., 2012). These models operate within a distributed framework to take physical and meteorological conditions of the basin into account (Refsgaard and Knudsen, 1996). Physically distributed models include both fully distributed and semi-distributed models. Owing to their extensive parameterization, fully distributed models are difficult to employ at a large catchment scale which make comparatively less data intensive semi-distributed models a practical alternative. This paper presents a simple hydrologic modelling based approach to isolate the impacts of land use and climate on streamflow. For this purpose, physically-based macroscale Variable Infiltration Capacity (VIC) hydrologic model (Liang et al., 1994) has been employed for the analysis.

In the present paper, Ganga river basin in India is selected as the case study to perform the analysis. Few studies have been reported in literature (Nijssen et al., 2001; Arora and Boer, 2001 and Nohara et al., 2006) wherein Ganga basin is studied alongside other major river basins of the world (to assess the effect of changing climate on flow regime), however, there is dearth of studies that comprehensively examine the effects of LU and climate change on streamflow exclusively in this basin. Originating from the Himalayas, the river Ganga traverses a stretch of 2525 km covering a catchment area of around 800,000 km<sup>2</sup> which is approximately 26% of the entire India's land mass making it the largest river basin in India. During its course, Ganga flows through some of the major states of India harboring about 44% of country's population (<http://censusindia.gov.in/>). Due to presence of alluvium, the basin is very fertile and forms close to 30% of India's cultivable area ([http://eands.dacnet.nic.in/LUS\\_2001-11.htm](http://eands.dacnet.nic.in/LUS_2001-11.htm)). Thus there is a clear consensus that the river is of great social and economic importance to India. In this study, the area under investigation is the upstream reaches of the Ganga basin encompassing river's originating place (Fig. 1). This region is referred as the Upper Ganga Basin (UGB) in the paper.

LU analysis carried out by Tsarouchi et al., (2014) on the UGB suggests that, between 1984 to 2010 basin experienced increase in urban and crop land area and decrease in barren land area.

In order to obtain the isolated impacts of LU and climate change on streamflow, following objectives are addressed in the current work: (i) assess sensitivity of the streamflow to changes in different LU categories, (ii) examine impacts of climate change on the streamflow and (iii) analyze integrated impacts of LU and climate change on the streamflow. The three objectives are translated into three scenarios wherein first two scenarios quantify the independent effects of LU and climate on streamflow under their invariant counterparts i.e., climate and LU respectively are kept constant. The third scenario deals with concurrent changes in LU and climate. Results from the three scenarios are further used to segregate the hydrologic impacts of LU and climate change. The aforementioned objectives are investigated over the UGB as a case study by employing a calibrated and validated VIC model to simulate streamflows. To assess the impact of future climate on streamflow in the basin, dynamically downscaled climate simulations for six GCMs obtained from the CORDEX project are used. Climate change related analyses are carried out under the uncertainty framework to address two issues, one, climate models based uncertainties, and two, emission scenarios based uncertainties.

## **2 Data and Methods**

### **2.1 Study Area**

The UGB, located within geographic coordinates of 25°30'N to 31°30'N latitude and 77°30'E to 80°E longitudes (Fig. 1), drains a catchment area of 95,593 km<sup>2</sup>. While most of the Ganga basin comprises of agricultural areas with reasonably flat terrain, this region (UGB) is the only part of the Ganga basin which is characterized by wide variation in topography with elevations ranging from 21 m to 7796 m (Fig. 1), thus making it an interesting case study for investigation. In addition, since the river Ganga originates in this region, any change in hydrologic response due to LU and /or climate is likely to affect the entire flow regime downstream. Thus this region is critical for assessing the impact of LU and climate change on the streamflow of the basin. In the backdrop of recent flood event in July 2013 in the UGB, which has been attributed to climate change (Singh et al., 2014), isolating the hydrologic impacts of changing LU and climate in this basin has become much more important.

In this study, the UGB is divided into three regions, upstream, midstream and downstream (Fig.1) based on altitude, topography and land use characteristics. The upstream region is highly mountainous, characterized by glaciers and dense forests having elevations from 297 m to 7796 m. From upstream to midstream region, there is transition from hills to plains. Midstream region is dominated by forests and crop lands with elevations ranging from 75 m to 3079 m. The downstream region is mostly covered by crop lands having consistent elevations of around 100 m. In addition to the varying land use characteristics, these three regions have different climatology as well. From 1971 to 2005, upstream, midstream and downstream regions recorded an average annual precipitation of 1294, 1009 and 826 mm respectively. Most of the precipitation is concentrated during the monsoon months from June to September (JJAS). Average annual temperatures across the three regions during the same period were 20°C, 23°C and 26°C respectively. Due to significant variation in the characteristics of these regions, they are modelled separately in the paper. Details of data required to drive the hydrologic model are presented in the following section.

## **2.2 Input Data for the Hydrologic Model**

The current study employs physically based Variable Infiltration Capacity (VIC) hydrologic model for the analysis. The VIC model is a semi-distributed soil-vegetation-atmosphere-transfer model that solves coupled water and energy balance equations grid wise to calculate different hydrologic components (Liang et al., 1994). Within a grid the VIC model considers sub-grid heterogeneity by dividing each grid cell into number of tiles which in turn depend on different land use types present in the grid. Each tile generates different response to the precipitation in the form of infiltration, soil moisture storage, runoff and evaporation, owing to difference in land surface properties. When VIC concludes the computation of energy and water balance calculations for each grid within the watershed, streamflow routing model developed by Lohmann et al., (1998) is activated that transports the surface runoff generated within a grid along with the baseflow to the outlet of grid cell which is further routed through the river channel to the watershed outlet.

Hydrologic models in general require topographic, soil, hydro-meteorological and LU data which can be procured from various sources. In the present work, topographic information is obtained from ASTER (Advanced Spaceborne Thermal Emission and Reflection Radiometer)

DEM (Digital Elevation Model) available at 30 m spatial resolution. Digital soil map for the region is procured from National Bureau of Soil Survey and Land Use Planning, India at a scale of 1:250,000. Meteorological data (rainfall, maximum temperature, minimum temperature and wind speed) for the period 1971-2005 at daily time scale is procured from two sources: Indian Meteorological Department (IMD) (Rajeevan et al., 2006) and Princeton University (PU) (Sheffield et al., 2006). Meteorological data from both the sources are brought to a common grid resolution of  $0.5^\circ$  which also serves as the resolution for executing the VIC hydrologic model. Observed streamflow data ( $Q_{obs}$ ) for two locations: Bhimgodha (1987-2011) and Ankinghat (1977-2009) is obtained (at monthly scale) from Uttar Pradesh Irrigation Department and Central Water Commission (CWC). Between Bhimgodha and Ankinghat stations, there are diversions such as Upper Ganga Canal (UGC), Madhya Ganga Canal (MGC) and Lower Ganga Canal (LGC) (Fig. 1) that divert the water from the main Ganga River. Therefore, along with  $Q_{obs}$ , data corresponding to various diversion channels is also procured from CWC and added to the observed (regulated) flow thereby converting the observed streamflow to naturalized flow ( $Q_{n-obs}$ ). The flow data thus obtained ( $Q_{n-obs}$ ) is used for model calibration and validation.

For LU data, landsat imageries for the years 1973, 1980, 2000 and 2011 are selected and then classified to determine the LU change in the basin over four decades. Field study is carried out to collect the training sites for image classification. The accuracy of classified images is obtained to be 89%, 83%, 88% and 79% for 1973, 1980, 2000 & 2011 images respectively which is seen to be generally good. Thus the classified images can be used as LU maps of the UGB for the corresponding time periods. Results of classification and change in LU are presented in section 3.1.

To carry out hydrologic impact studies related to climate change, one needs data on future climate variables such as rainfall ( $P$ ), temperature ( $T$ ) and wind speed ( $W$ ) which in the current study is procured from CORDEX South Asia group (<http://cccr.tropmet.res.in/cordex/index.jsp>) at daily scale for six Coupled Model Intercomparison Project 5 (CMIP5) GCM simulations (Table 1). Each model has a time series for all the requisite variables corresponding to the twentieth century climate (historic run) and future climate using Representative Concentration Pathway, RCP 4.5 and RCP 8.5 emission scenarios. All the GCM outputs are brought to a consistent resolution of  $0.5^\circ$ .

It is now well known that large scale pattern of climate variables simulated by GCMs may be realistic, but when downscaled to regional level, they may exhibit significant bias compared to the observed data (Maurer and Hidalgo, 2008; Ghosh and Mujumdar, 2009). This can have significant effect on hydrological impact studies which necessitates the need of performing bias correction on the climate variables obtained. In the current work, climate variables obtained from the GCMs are bias corrected with IMD gridded data (which is considered as observed data) at daily scale using the technique developed by Wood et al., (2002). A distribution function is fit to the observed daily data and individual GCM data.  $F_{GCM}(x)$  of a GCM simulation is identified for a given  $x$  and the corresponding observed value  $x'$  is obtained from the observed CDF,  $F_{obs}(x')$  such that  $F_{obs}(x') = F_{GCM}(x)$ . GCM value  $x$  is then replaced with the observed value  $x'$  on the CDF of GCM.

Statistics of GCM simulated (post bias correction) and observed climate variables for upstream region are presented in Taylor diagram (Fig. 2). It can be observed that all the models are clustered together which could be due to the fact that all the GCM outputs are from the same modelling center and, the clusters in case of  $T_{max}$  (maximum temperature) and  $T_{min}$  (minimum temperature) [Fig. 2 (b) & (c) respectively] are closer to the observed data (represented by point 'a') which reflects a better quality of GCM outputs for  $T$ . In case of  $P$  [Fig. 2 (a)], it is observed that the models' cluster is slightly far from point 'a', nevertheless, reasonably good correlation of 0.6-0.7 exists between GCM  $P$  and observed  $P$ . Similar inferences are drawn from the analyses over midstream and downstream regions.

In addition to the correlation coefficient, climatology of variables for different GCMs is compared with the climatology of the observed variable from 1971-2005 at monthly scale. These results are presented in Fig. 3 for one of the grid cells within the UGB. The observed and GCM climatology at monthly scale for time period 1971-2005 is represented following Wood et al. (2002). It can be observed from Fig. 3 that the GCMs successfully reproduce the mean and variance of the rainfall climatology for most of the months. However, for post-monsoon period (i.e. October, November and December) GCMs overestimate the rainfall compared to the observed rainfall. For  $T_{max}$  and  $T_{min}$ , (Fig. 3 B & C respectively) GCMs could successfully reproduce the observed climatology across all the months. Other grids within the UGB were found to demonstrate a similar pattern for both rainfall and temperature. Based on this analysis,



downscaled variables are considered to reasonably represent the climate of the region and are further used to drive the VIC model.

In addition to the meteorological data and LU information, VIC requires explicit information about the vegetation type in the study region. In the study area, it is observed from the agricultural statistics ([http://mospi.nic.in/Mospi\\_New/site/India\\_Statistics.aspx](http://mospi.nic.in/Mospi_New/site/India_Statistics.aspx)) that wheat is grown in abundance during the rabi season (October-March) while rice and millets are grown during the kharif season (July-October). Furthermore, sugarcane is also grown in the upstream region of the UGB. Therefore, vegetation parameters corresponding to these four crops are provided as input to the relevant grid cells within the UGB.

### **2.3 VIC Hydrologic Model: Calibration and Validation**

For the model calibration in the present work, three parameters as suggested by Lohmann et al., (1998) are calibrated to obtain an optimum combination such that the error between observed and simulated streamflow is minimum. The three parameters considered are (i)  $B$  - variable infiltration curve parameter; (ii)  $D_s$  - fraction of maximum velocity of baseflow where nonlinear baseflow begins; and (iii)  $W_s$  - fraction of maximum soil moisture where nonlinear baseflow occurs. According to Liang et al., (1994) the parameter  $B$  has largest effect on runoff hydrograph and  $D_s$  and  $W_s$  parameters are critical in influencing the baseflow. Calibration of these parameters is necessary since their values vary with catchments. Moreover, these are the only three parameters which are unknown in the present study. All the other parameters (<http://www.hydro.washington.edu/Lettenmaier/Models/VIC/Documentation/SoilParam.shtml>) are obtained from the soil map used in this study.

VIC model is established independently for upstream, midstream and downstream regions but model calibration became possible only for upstream and midstream regions since  $Q_{obs}$  is not available for the downstream region. To address this issue, utilizing the facts that the downstream region has soil type similar to that of midstream region (loam and sandy loam) and the three parameters are essentially influenced by soil, it is assumed that the calibrated parameters obtained for midstream will hold good for downstream region.

To perform model calibration, initially the sensitivity of the simulated discharge to each of the three parameters is tested and their rough estimate of range for both upstream and midstream

regions are obtained. Within this range, several candidate models for upstream and midstream regions are created based on several plausible combinations of these three parameters. The VIC model is executed for all the combinations and the one that has maximum predictive power in terms of coefficient of determination ( $R^2$ ), normalized root mean square error ( $E_{\text{NRMSE}}$ ), nash sutcliffe efficiency ( $E_{\text{NSE}}$ ) and bias ( $\beta$ ) for monthly series of simulated streamflow ( $Q_{\text{sim}}$ ) during calibration period is considered. Here, a negative value of  $\beta$  indicates that model overestimates the simulated data and vice versa. It is to be noted that, though the VIC model is executed at daily scale, daily  $Q_{\text{sim}}$  values are aggregated to monthly values to carry out comparison between  $Q_{\text{sim}}$  and  $Q_{\text{n-obs}}$  since  $Q_{\text{n-obs}}$  is available only at monthly scale.

For the current work, periods of 1987-1999 and 1977-1995 in the upstream and midstream regions respectively are considered for calibration. Figure 4 provides the plots of corresponding observed and calibrated VIC simulated monthly streamflow series for the two regions. It can be observed from Fig. 4 that simulations during the calibration period captured the observed pattern and magnitude of hydrograph very well. In particular, rising and recession limbs of hydrographs are simulated accurately for both the regions. Shortcomings in the VIC simulations for both the regions include mismatch of peak flows which could be due to errors in modelling extreme precipitation by the model. Since we are not dealing with extremes in the present case study, this error is not of much concern. In addition, it may also be observed that at the end of each recession limb, there is a sharp drop, which is below the level of  $Q_{\text{n-obs}}$ . It could be due to inconsideration of baseflow contribution from the ground water in  $Q_{\text{sim}}$  which needs to be included in Indian watersheds, wherein groundwater serves as major contributor to the streamflow in the form of baseflow during the months of November to March. Also, in the upstream region, some infrequent peaks are simulated by the model during low flow periods which can be attributed to the overestimation of snow melt runoff by the snow module (which is kept active) in the region. Pre and post monsoon rainfall events could also result in this kind of behavior.

The calibrated models are validated from 2000-2005 and from 1996-2005 for the upstream and midstream regions respectively (presented in Fig. 5). Streamflow pattern and magnitude of runoff are well simulated during validation. Table 2 presents optimum set of parameters for the two regions along with their performance measures during calibration and validation. Based on

the performance measures it is seen that model is able to predict  $Q_{n-obs}$  reasonably well. Slight negative  $\beta$  [which is evident from scatter plot of Fig. 4 (a)] is observed for upstream region which could be due to overestimation of low flow values. Positive  $\beta$  for midstream region could be due to lack of groundwater contribution to  $Q_{sim}$ . The rigorously calibrated and validated VIC model is used to simulate the streamflow under different scenarios considered in the present study.

## 2.4 GCM and Emission Scenario Uncertainty

Despite strong correlation between the model simulated and observed climate variables (Fig. 2), it is noticed that the magnitude of uncertainty across different models is quite large with respect to observed  $P$  and  $T$  at annual scale. These uncertainties may get manifested in the hydrologic response (Arnell, 2011) when the future projections are used to drive the VIC hydrologic model for impact assessment. As a result it is essential to quantify the uncertainties associated with both climate data and streamflow generated from the VIC model, which, in the present work, is carried out over six GCMs and two emission scenarios. The uncertainty is quantified with Root Mean Square Difference ( $\sigma$ ) metric given by Eq. (1) (Giorgi and Mearns, 2002; Ekström et al., 2007).

$$\sigma = \left[ \frac{1}{n} \sum_{i=1}^n (\Delta X_i - \overline{\Delta X})^2 \right]^{\frac{1}{2}} \quad (1)$$

where,  $n$  is the number of GCMs for a given RCP;  $X$  is variable under study;  $\Delta X_i$  is the change in the  $i^{th}$  model mean value from the mean of the baseline period of the variable  $X$ ;  $\overline{\Delta X}$  is the ensemble average of change in mean given by Eq. (2)

$$\overline{\Delta X} = \frac{1}{n} \sum_{i=1}^n \Delta X_i \quad (2)$$

In the present work,  $\overline{\Delta X}$  is considered as estimate of effect of climate change.  $\sigma$  quantifies the average deviation of change in individual model mean from ensemble average of change in mean. Higher the  $\sigma$ , more is the uncertainty associated with the  $\overline{\Delta X}$  and consequently less reliable are the results. Further, the ensemble mean of models is statistically analyzed with baseline period's mean to test for equality of means using two sampled t-test. The results of t-test

are interpreted in terms of confidence levels for the change in future projections with respect to baseline period.

In order to infer the confidence level in terms of climatology, classification considered by Maurer (2007) is used according to which, confidence level (i) >90% indicates a highly significant change;(ii) 67-90% indicates moderately significant change, and (iii) <67% indicates insignificant change. Furthermore, same test is used to estimate the confidence level with which it can be claimed that the two emission scenarios give statistically different ensemble means. Figure 6 presents the overview of the work.

### **3 Results and Discussion**

Sections 3.1 and 3.2 provide analysis pertaining to the quantification of changes observed in LU and climate. In section 3.3, these results are used to quantify streamflow variations within the uncertainty framework.

#### **3.1 Analysis of Land Use**

Classification of landsat imageries resulted in LU maps for the UGB which are presented in Fig. 7. It can be observed that the UGB exhibits wide variations in the LU wherein upstream parts are snow covered and downstream parts are crop land. The dominant LU type in the UGB is crop land which covers about 56% of the entire basin (45%, 53%, 64% and 66% for 1973, 1980, 2000 and 2011 respectively). Upon visual examination of figures, it is evident that from 1973 to 2011, area under forest in the upstream region has diminished significantly. Percentage of total basin area under different LU categories in the UGB for different time periods is provided in Table 3.

It should be noted that for the present study, detailed snow cover mapping is not performed. Thus the percentage area observed under snow category in Table 3 should not be considered as a trend in the snow cover of the region. Urban category is observed to occupy very less area in the basin (< 5%) across all the time periods. For dense forest area, a decline was observed from 1973 to 2000 followed by an increase. The reason could be attributed to better forest management strategies that are introduced in the region after creation of Uttarakhand state in November 2000. It is observed that there is slight increase in surface area of water which could be attributed to development of structures such as Ramganga reservoir (Fig. 1) after 1973. Results reflect that there has been a massive increase in the area under cultivation in the basin. The dynamics of LU

is heavily supported by rapid increase in population of the region (120% increase between 2001 and 2011 as per census of India, <http://censusindia.gov.in/>). The impact of changes in LU over streamflow is assessed in section 3.3.1. The following section provides analysis of climate change in the UGB.

### 3.2 Analysis of Climate Variables

Observed rainfall obtained from IMD and projections of rainfall ( $P$ ) obtained from GCMs are examined for long term trends using Mann Kendall test (Mann 1945; Kendall, 1938). It is noticed that observed  $P$  did not show any trend during the period 1971-2005 for upstream, midstream and downstream regions. However, projections of  $P$  exhibits a monotonic increase at the annual scale during the period 2010-2099 for all the regions with large inter annual variability. In order to determine the change in the climatology of the three regions, outputs from GCMs for future time period are aggregated into five time slices T1 (2010-2020), T2 (2021-2040), T3 (2041-2060), T4 (2061-2080) and T5 (2081-2100). Further on, comparisons are made between the means of the future time slices' and the baseline period (1971-2005). Figure 8 (top panel) shows average change in annual  $P$  over all GCMs ("ensemble mean change") in future time slices from the baseline period which is calculated using Eq. (2). Associated with the ensemble mean change is uncertainty, obtained using Eq. (1), which is represented by error bars in the figure. Uncertainty limits reflect the average deviation of change in the mean of individual GCMs from the ensemble mean.

T2 in case of RCP 4.5 emission scenario is observed to exhibit maximum change for all the three regions along with high uncertainties. High confidence level associated with T2 imply probable impacts in hydrologic response associated with this time slice. RCP 8.5 emission scenario, for most of the time slices, exhibits moderately significant change which may result in less probable impacts.

Upon assessing the monthly variability in  $P$ , it is observed that it may decline significantly during monsoon months whereas there might be an increase during winter months (October, November, December, January) across the three regions. This may result in shift in seasonal pattern of  $P$  in the region. Furthermore, if analyzed longitudinally from upstream to downstream it is noticed that the variation in  $P$  in downstream region is much more severe.

On analyzing the trend in observed and projected annual mean  $T_{\max}$  and  $T_{\min}$ , it is noticed that observed annual mean  $T_{\max}$  did not show any trend during 1971-2005, while observed annual mean  $T_{\min}$  depicted an increasing trend during the same period. However, projected annual mean  $T_{\max}$  and  $T_{\min}$ , are observed to show an increasing trend for future scenarios. Upon assessing the monthly variability, mean  $T_{\max}$  and  $T_{\min}$  are observed to increase significantly during winter months and they may decline during April to September in all the regions. Results corresponding to ensemble change in mean annual  $T_{\max}$  and  $T_{\min}$  from the baseline are shown in Fig. 8, center and bottom panels respectively. Change in  $T_{\max}$  and  $T_{\min}$  can affect the hydrology by changing rain to snow ratio, ET and consequently runoff (Christensen et al., 2004). Therefore, change in  $T$  may affect the overall water availability in the basin. On assessing the change in  $T$  longitudinally over UGB, it is observed that downstream region may experience maximum increase in the annual mean  $T_{\max}$  and  $T_{\min}$  thus causing serious implication in this part of the UGB. Downstream region, as mentioned earlier, may suffer from sporadic  $P$  along with significant increase in  $T$ , resulting in severe water availability problem in this part of the UGB. This condition may prove to be detrimental from agricultural point of view as this area is heavily under cultivation (86% of total downstream area).

Upon evaluating the emission scenario based uncertainty, it is found that there is no significant difference between the two scenarios RCP 4.5 and RCP 8.5 which indicates that the scenario based uncertainty will be minimum. Impacts of changes in  $P$  and  $T$  on streamflow are presented in section 3.3.2.

### **3.3 Hydrologic Responses to Land Use and Climate Change**

To evaluate the effects of land use (LU) and climate change on the hydrology of the study area, three scenarios are considered. The first two scenarios are based on the single factor approach (Li et al., 2009), i.e., one driving factor is changed at an instant keeping the other constant. In the first scenario, climate is considered invariant while LU is varied with time whereas in the second scenario, LU is considered invariant while climate is varied with time. These two scenarios are constructed to understand how streamflow would respond if only one of the driving forces is changed with time thereby assisting in quantifying the influence of individual factors on streamflow. In reality, both LU and climate change simultaneously with time and the hydrologic response is generated based on their integrated effect which is addressed by the third scenario.

Finally from the integrated response, contributions of LU and climate on the streamflow variability is segregated using results from the other two scenarios. In depth analysis in the first two scenarios is carried out due to lack of detailed studies that examine the effects of LU and climate change on streamflow in the UGB.

### **3.3.1 Impact of Land Use Change**

In order to investigate hydrological impacts of LU change, simulations are carried out keeping climate fixed at 1971 while LU is changed progressively from 1971 to 2011. LU in any region changes gradually over a period of time and therefore starting and ending years may satisfactorily represent the change that has occurred in each LU class. Considering this, LU of the intermittent years can be obtained using rate of change in each LU class between the starting and ending years. It is to be noted that to obtain LU information for 1971 and 1972, rate of change between 1973 and 1980 is considered. LU obtained for each year is then used to drive the VIC model to obtain simulations under LU effect with invariant climate. Although simulations are carried out continuously from 1971 to 2011, for the sake of brevity, results corresponding to the starting year (1971) and the ending year (2011) for all the three regions are presented in Fig. 9.

It can be observed from the Fig. 9 that from 1971 to 2011, there is an increase in the magnitude of peak discharge for the upstream and midstream regions. This observation is consistent with other studies reported in literature which state that LU change has pronounced effect on peak flows due to alterations in the infiltration capacity of the surface (Fohrer et al., 2001; Naef et al., 2002; Tollan, 2002; McIntyre et al., 2014). No change in the discharge regime of the downstream region is noticed. LU and topography of the region is observed to have a conspicuous effect on the hydrologic response from the basin which is reflected in the hydrograph patterns for the three regions. Rising limb of the upstream region [Fig. 9 (a)] begins during April while for midstream and downstream [Fig. 9 (b) & (c) respectively] it occurs during May-June. The early occurrence of rising limb in upstream region can be attributed to the snowmelt runoff contribution to the streamflow. However, for midstream and downstream regions, rising limb begins with the onset of monsoon. The recession limb of hydrograph for upstream region falls quickly owing to the steep slope of the region. For midstream, a sharp drop is observed up to a certain level during October indicating the termination of direct runoff

contribution to streamflow. Following this, the contribution is predominantly through baseflow which in this case is observed to be higher than the baseflow before the monsoon months. The higher baseflow during post monsoon period could be attributed to slow release of water stored by forests (dense and scrub) in the region aided by low elevation of the terrain in the region. Downstream region, though entirely a flat terrain, is dominated by crop land and urban areas that lack the capacity of holding the water, therefore limiting the contribution of baseflow to streamflow which leads to the observed sharp decline in recession limb. Furthermore, long term impacts of LU change are more evident in annual streamflow which is observed to increase by 12 %, 17% and 1% from 1971 to 2011 for upstream, midstream and downstream regions respectively.

Sensitivity of the region to different LU categories is assessed in separate simulations. In this case, simulations considering each LU class are performed and change in streamflow under each category is quantified. To quantify the magnitude of change in streamflow caused by change in LU, ratio between streamflow and LU is computed. The ratio is referred to as Runoff-LU ratio (*RL*) in the present study. The *RL* indicates the effect of 1% change in any LU category on streamflow and aids in identifying the significance of a particular LU class in determining the hydrologic response. Based on the ratios obtained, streamflow response (to a particular LU category) is classified under three categories: (i) highly sensitive if  $RL \geq 3$ . It indicates that a change of 1% in LU category results in the change of hydrologic response by atleast three times; (ii) moderately sensitive, ( $1 \leq RL \leq 2$ ); and (iii) insensitive, ( $0 < RL < 1$ ). Sign associated with the *RL* indicates the direction of change.

It can be observed from Table 4 that in the upstream region, *RL* is maximum for the urban area implying that the hydrologic response in this region is highly sensitive to the changes in urban area. It can be inferred that 1% change in the urban area results in 4% increase in the streamflow from the upstream region. The upstream region has significant portion of area under dense forest that has shown minor increase in the last decade (2000 to 2011) (Table 3). The simulated streamflow is observed to be moderately sensitive to this increase, though the observed impact is in the opposite direction, i.e., increase in forest results in decrease in streamflow. Furthermore, streamflow simulated from the upstream region is moderately sensitive to crop lands as well. Midstream region has crop land as the dominant LU type covering 53% of the area during 1971



and 81% of the area in 2011, streamflow is observed to be moderately sensitive to it. It is also observed that streamflow is moderately sensitive to urban area in this region. Though the downstream region is predominantly cultivated land (approximately 85% of the area), hydrologic response is observed to be moderately sensitive to changes in the urban area. High sensitivity of streamflow from the regions to urban area can be attributed to the fact that increase in urban sprawl could reduce the infiltration resulting in generation of higher surface runoff. In addition to this, it can be observed that hydrologic response to change in forest area in the midstream and downstream regions has a positive sign unlike in the upstream region, where the response has a negative sign. This is due to the fact that midstream and downstream regions are dominated by scrub forest, area under which has decreased over the time period, thereby increasing the streamflow. Thus all the three regions of the UGB are observed to be moderately sensitive to change in crop land area while moderately to highly sensitive to change in urban area.

### 3.3.2 Impact of Climate Change

Streamflow observed at Bhimgodha (outlet for upstream region) and Ankinghat (outlet for the midstream region) stations is examined for the presence of trend using Mann-Kendall test. It is noticed that the observed streamflow for upstream (1987-2005) and midstream (1977-2005) regions do not show any trend. However, in order to investigate the individual impact of changing climate on hydrology, simulations are carried out keeping LU fixed for 1971 and altering climate continuously for the baseline period (1971-2005) and future emission scenarios (2010-2100). The simulation results obtained are referred to as  $Q_{\text{clim}}$  hereafter. To quantify the change in streamflow, the VIC model is driven using the downscaled, bias-corrected six GCM outputs and the simulation results obtained are compared with the baseline simulation results. Change in ensemble mean annual  $Q_{\text{clim}}$  for five future time slices from the baseline annual streamflow for the three regions is presented in Fig. 10 with the associated uncertainties shown as error bars.

From the Fig. 10, it can be observed that change in  $Q_{\text{clim}}$  has patterns similar to that of change in mean annual  $P$  (Fig. 8, top panel). Change in  $Q_{\text{clim}}$  for all the time slices is observed to be moderate to highly significant in most of the cases indicating probable impacts of climate change on hydrologic response of the basin. Uncertainty is observed to increase through the time slices and maximum uncertainty in projection results for all the three regions is observed in T5.

Although the two scenarios gave consistent results, to address the issue of scenario based uncertainty, mean of ensemble annual  $Q_{\text{clim}}$  series of RCP 4.5 is compared with mean of ensemble annual  $Q_{\text{clim}}$  series of RCP 8.5. The two means are found to be moderately different for the midstream region, indicating the need to consider the two scenarios as separate cases.

Assessment of the monthly variations in the  $Q_{\text{clim}}$  across future time slices indicated that  $Q_{\text{clim}}$  may decrease for JAS months for the three regions while it may increase during the months of October, November and December (OND). The variations observed in  $Q_{\text{clim}}$  during JAS and OND are found to be consistent with that of  $P$ . However, this is not true for all the months such as June, where  $P$  is observed to decrease in future while  $Q_{\text{clim}}$  is observed to increase which can be attributed to decrease in  $T$  that may reduce evaporation from the region resulting in higher runoff. Similar kind of response of streamflow to  $P$  and  $T$  in a catchment is reported in literature for a different case study by Fu et al. (2007). To further assess the sensitivity of  $Q_{\text{clim}}$  to changes in  $P$  and  $T$  and quantify their effect, runoff ratio ( $RR$ ) is computed using average annual runoff and rainfall for each time slice. Results pertaining to the values of  $RR$  are presented in Table 5.

The  $RR$  is a simple index that reflects the relationship between  $P$  and  $Q_{\text{clim}}$  by determining the proportion of  $P$  that gets converted to  $Q_{\text{clim}}$  (Zhang et al., 2011).  $RR$  is calculated by normalizing the  $Q_{\text{clim}}$  with  $P$  within the same time scale. Analyzing  $RR$  over a period of time on the same river basin (under same LU conditions) aids in understanding topographic response and effect of climate on streamflow. In the present study, longitudinal variation in  $RR$  strikingly depicts the catchment topography from upstream to downstream.  $RR$  is observed to be 60% for the upstream region, 44% for the midstream region and 23% for the downstream region during the baseline period. Upstream region is characterized by mountainous terrain and steep slopes thus most of the  $P$  gets converted to  $Q_{\text{clim}}$  (high  $RR$ ), whereas downstream region has very flat terrain thus much of the  $P$  get evaporated or infiltrated into soil and little gets converted to  $Q_{\text{clim}}$  (low  $RR$ ). Analysis of  $RR$  over the different time slices for a particular region indicate that in general, when  $P$  does not change significantly from the baseline period, increase in  $T$  results in reduced  $RR$ . This is intuitive as increase in  $T$  leads to loss of water as evaporation which reduces  $Q_{\text{clim}}$  and consequently lessens  $RR$ . The  $RR$  is observed to increase and approach towards baseline  $RR$  with slight increase in  $P$  (irrespective of change in  $T$ ). In such cases, temperature variations are seen to be of less importance. In most of the cases it is observed that decrease in  $P$  results in decrease in

$RR$ , but in few cases such as T4 and T5 (RCP 4.5 and RCP 8.5) for downstream region,  $P$  is observed to reduce accompanied by an increase in  $T$ . In such a case, one might expect  $RR$  to reduce significantly which is not observed. This anomaly could be attributed to occurrence of short duration dense rainfall events in the region. Reduction in  $RR$  is observed in case when  $P$  is observed to increase with no significant change in  $T$ . This kind of behavior could be due to shift in seasonal pattern of  $P$  or due to increased inter-arrival time between the two  $P$  events. In summary,  $Q_{clim}$  from the downstream region is observed to be very sensitive to the changes in  $P$  whereas  $Q_{clim}$  is sensitive to  $P$  up to a certain threshold for midstream region, beyond which  $T_{max}$  also starts playing a role. Owing to the complex topography and climatology of the upstream region, it is difficult to interpret the sensitivity of  $Q_{clim}$  to different climate factors.

### 3.3.3 Integrated Impacts of Land Use and Climate Change

In a real world situation, change in LU and climate occurs simultaneously and the impact of both these factors is reflected in the streamflow. To carry out analysis pertaining to this scenario, one needs concurrent information on LU and climate. Under this notion, VIC model is driven for 1971-2005 (baseline period) across the three region in the UGB. It is to be noted that the process of obtaining projections of future LU conditions in the basin does not come under the purview of present work. Therefore, integrated impact of LU and climate change on future streamflow could not be assessed. The results obtained from this analysis can be interpreted as the streamflow simulations under simultaneous change in LU and climate conditions (hereafter referred to as  $Q_{int}$ ). In order to assess decadal variations in streamflow of the UGB, baseline period is aggregated to four time periods: P1 (1971-1980); P2 (1981-1990); P3 (1991-2000) and P4 (2001-2005), although, VIC model is executed for the entire duration. Results corresponding to  $Q_{int}$  for upstream, midstream and downstream regions are presented in Table 6. It is observed that no clear inference about the implication of LU and climate on streamflow can be achieved from the obtained  $Q_{int}$  values due to large variability in the streamflow corresponding to the variability in rainfall. Therefore a further analysis is necessary to isolate the impacts of LU and climate on streamflow response which is presented in the following sub-section.

### 3.3.4 Isolating the Impacts of Land Use and Climate

In order to segregate the impacts of LU and climate, the proposed approach primarily requires results of  $Q_{int}$  (obtained from the section 3.3.3), and  $Q_{clim}$  (obtained from the section 3.3.2) over

the same time period. Herein  $Q_{\text{int}}$  and  $Q_{\text{clim}}$  are comparable based on the fact that the respective simulations are obtained under identical conditions of hydrologic model and climatology. This condition reflects that the only changing subject among the two scenarios is the land use input to the hydrologic model. Therefore, the residue of the two scenarios,  $Q_{\text{int}} - Q_{\text{clim}}$ , is considered to be the exclusive contribution of LU to streamflow (hereafter referred to as  $Q_{\text{LU}}$ ). To segregate the contribution of LU and climate from  $Q_{\text{int}}$ , a linear response of LU and climate to the streamflow is assumed.

In the present case study, simulations of  $Q_{\text{int}}$  and  $Q_{\text{clim}}$  are obtained for the time periods P1, P2, P3 and P4 mentioned earlier for upstream, midstream and downstream regions.  $Q_{\text{int}}$  and  $Q_{\text{clim}}$  are then used to estimate  $Q_{\text{LU}}$ . Alongside, the percentage contributions of LU and climate to  $Q_{\text{int}}$  are

also computed ( $Q_{\text{clim (LU)}} (\%) = \frac{Q_{\text{clim (LU)}}}{Q_{\text{int}}} \times 100$ ). Table 6 presents results pertaining to these.

Results from Table 6 suggest that climate is the dominant contributor to streamflow across all the regions. Contribution of LU, on the other hand, is observed to be minimal. Further insight to the influence of LU to streamflow is obtained from the inferences drawn from section 3.3.1. It is observed from the analysis in section 3.3.1 that streamflow is highly sensitive to changes in urban land in upstream and downstream regions while it is moderately sensitive to urban and crop land areas in midstream region. The spatial extent of urban area is observed to be very less in the upstream and downstream regions (less than 10%), which could have resulted in negligible contribution of LU to streamflow. For the midstream region, despite ~70% of the area is under crop land, contribution of LU to streamflow turned out to be less. This could be due to moderate sensitivity of streamflow to the changes in crop land category. It is well understood that crop lands contribute more to the ET than to the streamflow. Contribution of urban area to streamflow is negligible due to its less spatial extent in the midstream region. When  $Q_{\text{LU}} (\%)$  is assessed across the time periods in the three regions, it is observed that there is gradual increase in the contribution of LU to streamflow. This could be attributed to the fact that area under the sensitive LU categories (urban area and crop land) is increasing with time in the regions.

Contribution of LU and climate on the streamflow response is isolated at the monthly scale as well. It is observed that climate is major contributor to the streamflow across all the three regions at monthly scale as well (Pl. see the attached supplement).

In the present study, the application of proposed methodology of isolating the hydrologic impacts of LU and climate is limited only to the baseline period due to unavailability of future LU information. However, this approach can be applied to the future time periods as well upon obtaining future LU projections along with climate simulations. This is illustrated by conducting the analysis on T1 (2010-2020) wherein  $Q_{int}$  is obtained by driving VIC model under LU condition of 2011 (assuming that LU may not change significantly during this decade) and climate simulations from six GCMs for the corresponding time period. Results for the T1 are presented in Table 7.

From Table 7, it can be observed that the contribution of LU to streamflow from upstream region has increased (compared to P4). This could be attributed to increase in area under urban land by 65% in T1 from P4 in the upstream region. No significant increase is observed in crop land and urban land areas in T1 from P4 for midstream and downstream regions respectively (2% increase in crop land in midstream region and 20% increase in urban area in downstream region) which could have resulted in unvarying contribution of LU to streamflow from P4 (Table 6) to T1 (Table 7) in these regions.

From the analysis, it can be concluded that the proposed approach can be applied over a catchment with a well calibrated and validated hydrologic model. Future work involves generating LU projections for future time periods which can be corroborated with climate projections described in section 3.3.2 to isolate the impacts of LU and climate on future streamflow simulations. Although there is presence of snow covered region in the basin, segregating the contribution of snow melt runoff from the total streamflow is not feasible at this stage due to lack of observed data. This limits the assessment of impact of temperature changes on snow melt and its consequences on the streamflow.

#### **4 Conclusions**

In the present paper a hydrologic modelling based methodology is presented to isolate the impacts of LU and climate on streamflow in a river basin. To achieve this, three objectives are considered (i) assessing the sensitivity of the streamflow to the changes in LU (ii) examining the impact of change in climate on the streamflow and (iii) integrated impact of LU and climate change on the streamflow of the UGB. These three objectives are translated to three scenarios and are used to segregate the influence of LU and climate change on the streamflow. Not many

studies conducted earlier have considered the combined effect of LU and climate on the hydrology of the basin. The VIC hydrologic model is used to understand the impact of LU and climate change on the streamflow. The VIC model, owing to its comprehensive ability to simulate hydrological processes, has been used widely to perform impact assessment studies. However, being a physically based distributed model, there are concerns associated with the model structure and the number of calibration parameters. Furthermore, due to spatio-temporal variability in the input variables, parameter set for the initial or reference time period may not be suitable for future period (Viney et al., 2009). In the present study, these issues of concerns are partially addressed by calibrating and validating the VIC model over the upstream, midstream and downstream regions of the UGB.

LU change analysis of the study region indicated an increase in the areas of crop and urban land categories to which streamflow is observed to be moderately to highly sensitive. From the climate change analysis it is observed that rainfall may decrease during the monsoon months and increase during the winter months which may result in shift in seasonal rainfall pattern. Annual means of  $T_{\max}$  and  $T_{\min}$  are observed to increase in the future. Streamflow is observed to reproduce the variations in rainfall. All the changes in rainfall,  $T_{\max}$  and  $T_{\min}$  pertaining to climate change scenario are found to be statistically significant from the baseline period, indicating that deviation in their magnitudes is likely to cause serious impacts on the hydrologic response. It may be noted that the meteorological variables from only six GCMs are used for the analysis, which is a limitation of the study. There is a need to consider more GCMs to address the issue of model and scenario based uncertainty more comprehensively.

The integrated effect of LU and climate change on streamflow is observed to be more prominent in the study area. From the analysis of isolating the individual impacts of LU and climate from their integrative effects on streamflow, it is observed that climate contributes more to the simulated streamflow (>90%). In contrast, LU did not contribute significantly to the simulated streamflow which could be attributed to less spatial extent of sensitive LU categories in the region.

The proposed approach is generic and applicable to any river basin to isolate the relative impacts of LU and climate change on streamflow. However, the approach is based on the assumption of

linear response of LU and climate to the streamflow. The case study analysis indicates that the change in climate may become a major concern in the UGB for water resources management.

## Acknowledgments

The authors would like to thank Thomas Kjeldsen (manuscript handling editor), Ge Sun, Young-Oh Kim and the anonymous referees for providing very useful comments on the manuscript. The work is carried out as part of the MoES-NERC Changing Water Cycle (South Asia) project: Hydro-meteorological feedbacks and changes in water storage and fluxes in Northern India (grant number: MoES/NERC/16/02/10 PC-II). Authors acknowledge the support of Indian Meteorological Department (IMD) and Indian Institute of Tropical Meteorology (IITM) for providing the data.

## References

- Arnell, N. W.: Uncertainty in the relationship between climate forcing and hydrological response in UK catchments, *Hydrol. Earth Syst. Sci.*, 15, 897–912, doi:10.5194/hess-15-897-2011.
- Arora, V.K., and Boer, G.J.: Effects of simulated climate change on the hydrology of major river basins, *J. Geophys. Res.-Atmos.*, 106, 3335–3348, doi: 10.1029/2000JD900620, 2001.
- Beyene, T., Lettenmaier, D. P., and Kabat, P.: Hydrologic impacts of climate change on the Nile River Basin: implications of the 2007 IPCC scenarios, *Climatic Change*, 100, 433–461, doi:10.1007/s10584-009-9693-0, 2010.
- Christensen, N. S., and Lettenmaier, D. P.: A multimodel ensemble approach to assessment of climate change impacts on the hydrology and water resources of the Colorado River Basin, *Hydrol. Earth Syst. Sci.*, 11, 1417–1434, doi:10.5194/hess-11-1417-2007, 2007.
- Christensen, N. S., Wood, A. W., Voisin, N., Lettenmaier, D. P., and Palmer, R. N.: The effects of climate change on the hydrology and water resources of the Colorado River basin, *Climatic Change*, 62, 337–363, doi:10.1023/B:CLIM.0000013684.13621.1f, 2004.
- Cuo, L., Zhang, Y., Gao, Y., Hao, Z., and Cairang, L.: The impacts of climate change and land cover/use transition on the hydrology in the upper Yellow River Basin, China, *J. Hydrol.*, 502, 37–52, doi:10.1016/j.jhydrol.2013.08.003, 2013.
- Ekstrom, M., Jones, P. D., Fowler, H. J., Lenderink, G., Buishand, T. A., and Conway, D.: Regional climate model data used within the SWURVE project – 1: projected changes in seasonal patterns and estimation of PET, *Hydrol. Earth Syst. Sci.*, 11, 1069–1083, doi:10.5194/hess-11-1069-2007, 2007.
- Fohrer, N., Haverkamp, S., Eckhardt, K., and Frede, H. G.: Hydrologic response to land use changes on the catchment scale, *Phys. Chem. Earth Pt. B*, 26, 577–582, doi:10.1016/S1464-1909(01)00052-1, 2001.

661 Fu, G., Charles, S. P., and Chiew, F. H. S.: A two-parameter climate elasticity of streamflow  
 662 index to assess climate change effects on annual streamflow, *Water Resour. Res.*, 43, W11419,  
 663 doi:10.1029/2007wr005890, 2007.

664 Ghosh, S., and Mujumdar, P. P.: Climate change impact assessment: Uncertainty modeling with  
 665 imprecise probability, *J. Geophys. Res.-Atmos.*, 114, D18113, doi:10.1029/2008jd011648, 2009.

666 Giorgi, F., and Mearns, L. O.: Calculation of average, uncertainty range, and reliability of  
 667 regional climate changes from AOGCM simulations via the "reliability ensemble averaging"  
 668 (REA) method, *J. Climate*, 15, 1141–1158, doi:10.1175/1520-  
 669 0442(2002)015<1141:coaura>2.0.co;2, 2002.

670 Gleick, P. H.: Methods for evaluating the regional hydrologic impacts of global climatic  
 671 changes, *J. Hydrol.*, 88, 97–116, doi:10.1016/0022-1694(86)90199-X, 1986.

672 Guo, H., Hu, Q., and Jiang, T.: Annual and seasonal streamflow responses to climate and land-  
 673 cover changes in the Poyang Lake basin, China, *J. Hydrol.*, 335, 106–122, doi:  
 674 10.1016/j.jhydrol.2008.03.020, 2008.

675 Hamlet, A. F., and Lettenmaier, D. P.: Effects of climate change on hydrology and water  
 676 resources in the Columbia River basin, *J. Am. Water Resour. As.*, 35, 1597–1623,  
 677 doi:10.1111/j.1752-1688.1999.tb04240.x, 1999. Islam, S. A., Bari, M. A., and Anwar, A. H. M.  
 678 F.: Hydrologic impact of climate change on Murray–Hotham catchment of Western Australia: a  
 679 projection of rainfall–runoff for future water resources planning, *Hydrol. Earth Syst. Sci.*, 18,  
 680 3591–3614, doi:10.5194/hess-18-3591-2014, 2014.

681 Kendall, M. G.: A new measure of rank correlation, *Biometrika*, 30, 81–93, 1938.

682 Li, Z., Liu, W.-z., Zhang, X.-c., and Zheng, F.-l.: Impacts of land use change and climate  
 683 variability on hydrology in an agricultural catchment on the Loess Plateau of China, *J. Hydrol.*,  
 684 377, 35–42, doi:10.1016/j.jhydrol.2009.08.007, 2009.

685 Liang, X., Lettenmaier, D. P., Wood, E. F., and Burges, S. J.: A simple hydrologically based  
 686 model of land-surface water and energy fluxes for general-circulation models, *J. Geophys. Res.-*  
 687 *Atmos.*, 99, 14415–14428, doi:10.1029/94jd00483, 1994.

688 Lohmann, D., Raschke, E., Nijssen, B., and Lettenmaier, D. P.: Regional scale hydrology: I.  
 689 Formulation of the VIC-2L model coupled to a routing model, *Hydrolog. Sci. J.*, 43, 131–141,  
 690 doi:10.1080/02626669809492107, 1998.

691 Lørup, J. K., Refsgaard, J. C., and Mazvimavi, D.: Assessing the effect of land use change on  
 692 catchment runoff by combined use of statistical tests and hydrological modelling: case studies  
 693 from Zimbabwe, *J. Hydrol.*, 205, 147–163, doi: 10.1016/S0168-1176(97)00311-9, 1998.

694 Mango, L. M., Melesse, A. M., McClain, M. E., Gann, D., and Setegn, S. G.: Land use and  
 695 climate change impacts on the hydrology of the upper Mara River Basin, Kenya: results of a  
 696 modeling study to support better resource management, *Hydrol. Earth Syst. Sci.*, 15, 2245–2258,  
 697 doi:10.5194/hess-15-2245-2011, 2011.

698 Mann, H. B.: Nonparametric tests against trend, *Econometrica*, 13, 245–259,  
 699 doi:10.2307/1907187, 1945.



700 Maurer, E. P.: Uncertainty in hydrologic impacts of climate change in the Sierra Nevada,  
 701 California, under two emissions scenarios, *Climatic Change*, 82, 309–325, doi:10.1007/s10584-  
 702 006-9180-9, 2007.

703 Maurer, E. P., and Hidalgo, H. G.: Utility of daily vs. monthly large-scale climate data: an  
 704 intercomparison of two statistical downscaling methods, *Hydrol. Earth Syst. Sci.*, 12, 551–563,  
 705 doi:10.5194/hess-12-551-2008, 2008.

706 McIntyre, N., Ballard, C., Bruen, M., Bulygina, N., Buytaert, W., Cluckie, I., Dunn, S., Ehret,  
 707 U., Ewen, J., Gelfan, A., Hess, T., Hughes, D., Jackson, B., Kjeldson, T., Merz, R., Park, J.,  
 708 O’Connell, E., O’Donnell, G., Oudin, L., Todini, E., Wagener, T., Wheeler, H.: Modelling the  
 709 hydrological impacts of rural land use change, *Hydrology Research*, 45, 737–754,  
 710 doi:10.2166/nh.2013.145, 2014.

711 Naef, F., Scherrer, S., and Weiler, M.: A process based assessment of the potential to reduce  
 712 flood runoff by land use change, *J. Hydrol.*, 267, 74–79, doi: 10.1016/S0022-1694(02)00141-5,  
 713 2002.

714 Nijssen, B., O’Donnell, G. M., Hamlet, A. F., and Lettenmaier, D. P.: Hydrologic sensitivity of  
 715 global rivers to climate change, *Climatic Change*, 50, 143–175, doi:10.1023/a:1010616428763,  
 716 2001.

717 Nohara, D., Kitoh, A., Hosaka, M., and Oki, T.: Impact of climate change on river discharge  
 718 projected by multimodel ensemble, *J. Hydrometeorol.*, 7, 1076–1089, doi:  
 719 <http://dx.doi.org/10.1175/JHM531.1>, 2006.

720 Oki, T., and Kanae, S.: Global hydrological cycles and world water resources, *Science*, 313,  
 721 1068–1072, doi:10.1126/science.1128845, 2006.

722 Ott, B., and Uhlenbrook, S.: Quantifying the impact of land-use changes at the event and  
 723 seasonal time scale using a process-oriented catchment model, *Hydrol. Earth Syst. Sci.*, 8, 62–78,  
 724 doi:10.5194/hess-8-62-2004, 2004.

725 Rajeevan, M., Bhate, J., Kale, J. A., and Lal, B.: High resolution daily gridded rainfall data for  
 726 the Indian region: Analysis of break and active monsoon spells, *Curr. Sci. India*, 91, 296–306,  
 727 2006.

728 Refsgaard, J. C., and Knudsen, J.: Operational validation and intercomparison of different types  
 729 of hydrological models, *Water Resour. Res.*, 32, 2189–2202, doi:10.1029/96wr00896, 1996.

730 Renner, M., Seppelt, R., and Bernhofer, C.: Evaluation of water-energy balance frameworks to  
 731 predict the sensitivity of streamflow to climate change, *Hydrol. Earth Syst. Sci.*, 16, 1419–1433,  
 732 doi:10.5194/hess-16-1419-2012, 2012.

733 Renner, M., Brust, K., Schwaerzel, K., Volk, M., and Bernhofer, C.: Separating the effects of  
 734 changes in land cover and climate: a hydro-meteorological analysis of the past 60 yr in Saxony,  
 735 Germany, *Hydrol. Earth Syst. Sci.*, 18, 389–405, doi:10.5194/hess-18-389-2014, 2014.

736 Rientjes, T. H. M., Haile, A. T., Kebede, E., Mannaerts, C. M. M., Habib, E., and Steenhuis, T.  
 737 S.: Changes in land cover, rainfall and stream flow in Upper GilgelAbbay catchment, Blue Nile  
 738 basin-Ethiopia, *Hydrol. Earth Syst. Sci.*, 15, 1979–1989, doi:10.5194/hess-15-1979-2011, 2011.

739 Rose, S., and Peters, N. E.: Effects of urbanization on streamflow in the Atlanta area (Georgia,  
740 USA): a comparative hydrological approach, *Hydrol. Process.*, 15, 1441–1457,  
741 doi:10.1002/hyp.218, 2001.

742 Scanlon, B. R., Jolly, I., Sophocleous, M., and Zhang, L.: Global impacts of conversions from  
743 natural to agricultural ecosystems on water resources: Quantity versus quality, *Water Resour.*  
744 *Res.*, 43, W03437, doi:10.1029/2006wr005486, 2007.

745 Sheffield, J., Goteti, G., and Wood, E. F.: Development of a 50-year high-resolution global  
746 dataset of meteorological forcings for land surface modeling, *J. Climate*, 19, 3088–3111, doi:  
747 10.1175/JCLI3790.1, 2006.

748 Singh, D., Horton, D. E., Tsiang, M., Haugen, M., Ashfaq, M., Mei, R., Rastogi, D., Johnson, N.  
749 C., Charland, A., Rajaratnam, B., and Diffenbaugh, N. S Severe precipitation in northern india in  
750 june 2013: causes, historical context, and changes in probability, *B. Am. Meteorol. Soc.*, 95,  
751 S58–S61, 2014.

752 Tollan, A.: Land-use change and floods: what do we need most, research or management?, *Water*  
753 *Sci. Technol.*, 45, 183–190, 2002.

754 Tsarouchi, G., Mijic, A., Mould, S., and Buytaert, W.: Historical and future land-cover changes  
755 in the Upper Ganges basin of India, *Int. J. Remote Sens.*, 35, 3150–3176,  
756 doi:10.1080/01431161.2014.903352, 2014.

757 Viney, N. R., Bormann, H., Breuer, L., Bronstert, A., Croke, B. F. W., Frede, H., Gräff, T.,  
758 Hubrechts, L., Huisman, J. A., Jakeman, A. J., Kite, G. W., Lanini, J., Leavesley, G.,  
759 Lettenmaier, D. P., Lindström, G., Seibert, J., Sivapalan, M., and Willems, P.: Assessing the  
760 impact of land use change on hydrology by ensemble modelling (LUCHEM) II: Ensemble  
761 combinations and predictions, *Adv. Water Resour.*, 32, 147–158,  
762 doi:10.1016/j.advwatres.2008.05.006, 2009.

763 Vörösmarty, C. J., Green, P., Salisbury, J., and Lammers, R. B.: Global water resources:  
764 Vulnerability from climate change and population growth, *Science*, 289, 284–288,  
765 doi:10.1126/science.289.5477.284, 2000.

766 Wada, Y., van Beek, L. P. H., and Bierkens, M. F. P.: Modelling global water stress of the recent  
767 past: on the relative importance of trends in water demand and climate variability, *Hydrol. Earth*  
768 *Syst. Sci.*, 15, 3785–3808, doi:10.5194/hess-15-3785-2011, 2011.

769 Wagner, P. D., Kumar, S., and Schneider, K.: An assessment of land use change impacts on the  
770 water resources of the Mula and Mutha Rivers catchment upstream of Pune, India, *Hydrol. Earth*  
771 *Syst. Sci.*, 17, 2233–2246, doi:10.5194/hess-17-2233-2013, 2013.

772 Wang, D., and Hejazi, M.: Quantifying the relative contribution of the climate and direct human  
773 impacts on mean annual streamflow in the contiguous United States, *Water Resour. Res.*, 47,  
774 W00J12, doi:10.1029/2010WR010283, 2011.

775 Wang, G. Q., Zhang, J. Y., Jin, J. L., Pagano, T. C., Calow, R., Bao, Z. X., Liu, C. S., Liu, Y. L.,  
776 and Yan, X. L.: Assessing water resources in China using PRECIS projections and a VIC model,  
777 *Hydrol. Earth Syst. Sci.*, 16, 231–240, doi:10.5194/hess-16-231-2012, 2012.

- 778 Wang, S., Kang, S., Zhang, L., and Li, F.: Modelling hydrological response to different land-use  
779 and climate change scenarios in the Zamu River basin of northwest China, *Hydrol. Process.*, 22,  
780 2502–2510, doi:10.1002/hyp.6846, 2008.
- 781 Wang, S., Zhang, Z., McVicar, T. R., Guo, J., Tang, Y., and Yao, A.: Isolating the impacts of  
782 climate change and land use change on decadal streamflow variation: Assessing three  
783 complementary approaches, *J. Hydrol.*, 507, 63–74, doi:10.1016/j.jhydrol.2013.10.018, 2013.
- 784 Wood, A. W., Maurer, E. P., Kumar, A., and Lettenmaier, D. P.: Long-range experimental  
785 hydrologic forecasting for the eastern United States, *J. Geophys. Res.-Atmos.*, 107, ACL 6-1–  
786 ACL 6-15, doi:10.1029/2001jd000659, 2002.
- 787 Zhang, Y., Guan, D., Jin, C., Wang, A., Wu, J., and Yuan, F.: Analysis of impacts of climate  
788 variability and human activity on streamflow for a river basin in northeast China, *J. Hydrol.*, 410,  
789 239–247, 2011.
- 790 Zhang, X., Zhang, L., Zhao, J., Rustomji, P., and Hairsine, P.: Responses of streamflow to  
791 changes in climate and land use/cover in the Loess Plateau, China, *Water Resour. Res.*, 44,  
792 W00A07, doi:10.1029/2007WR006711, 2008.

793

**Table 1.** GCMs from the CORDEX project used in the present study

Modeling Center- Experiment Name	Driving GCM (Abbreviation)	Institution
Commonwealth Scientific and Industrial Research Organization, (CSIRO) Australia CCAM	ACCESS1.0 (ACC) CNRM-CM5 (CNR) CCSM4 (CCS) GFDL-CM3 (GFD) MPI-ESM-LR (MPI) NorESM1-M (NOR)	CSIRO Centre National de Recherches Meteorologiques National Center for Atmospheric Research Geophysical Fluid Dynamics Laboratory Max Planck Institute for Meteorology (MPI-M) Norwegian Climate Centre

794

795 **Table 2.** Structure of VIC model obtained for the upstream and midstream region along with the  
796 performance measures during calibration and validation phase

Region	No. of candidate models	Value of optimum set of parameters	Calibration				Validation			
			$R^2$	$E_{NRMSE}$	$E_{NSE}$	$\beta$	$R^2$	$E_{NRMSE}$	$E_{NSE}$	$\beta$
Upstream	47	$B=0.13;$ $Ds=0.0005; Ws=0.76$	0.77	0.23	0.77	-0.02	0.83	0.29	0.79	-0.18
Midstream	80	$B=0.044;$ $Ds=0.0004;$ $Ws=0.62$	0.88	0.14	0.86	0.12	0.71	0.47	0.53	-0.04

797

**Table 3.** LU analysis of UGB for years 1973, 1980, 2000 and 2011

Category	Area (% of total area of 95,593 km <sup>2</sup> )			
	1973	1980	2000	2011
Snow	9.5	10.4	6.5	5.5
Dense Forest	14.5	12.8	11.4	14.8
Scrub Forest	23.6	14.8	13.9	9.0
Crop Land	45.1	53.2	64.3	66.2
Barren Land	5.0	6.4	0.6	0.2
Urban Area	1.5	1.6	2.3	3.2
Water	0.7	0.9	1.0	1.1

800 **Table 4.** Runoff-LU ratio for different LU categories for upstream, midstream and downstream  
801 regions

Region	LU classes			
	Crop Land	Urban	Forest	Barren
Upstream	2.05	4.02	-1.31	0.91
Midstream	1.49	1.17	0.1	0.97
Downstream	0.63	2.69	0.9	0.93

802

803  
804

**Table 5.** Runoff Ratio across time slices for upstream, midstream and downstream regions  
(terms in parentheses indicate the percent change from the baseline values)

Region	Time Period	Rainfall (mm)		Runoff (mm)		Runoff Ratio	
		RCP 4.5	RCP 8.5	RCP 4.5	RCP 8.5	RCP 4.5	RCP 8.5
Upstream	Baseline	1294	1294	772	772	0.60	0.60
	T1	1196±172 (-8)	1210±46 (-7)	697±84 (-10)	683±32 (-12)	0.58 (-2)	0.56 (-4)
	T2	1084±480 (-16)	1257±43 (-3)	619±287 (-20)	715±30 (-7)	0.57 (-3)	0.57 (-3)
	T3	1377±171 (+6)	1323±32 (+2)	816±137 (+6)	771±26 (0)	0.59 (-1)	0.58 (-2)
	T4	1416±198 (+9)	1357±42 (+5)	845±163 (+9)	800±38 (+4)	0.60 (0)	0.59 (-1)
	T5	1424±182 (+10)	1405±27 (+9)	854±148 (+11)	842±26 (+9)	0.60 (0)	0.60 (0)
Midstream	Baseline	1009	1009	441	441	0.44	0.44
	T1	844±84 (-16)	871±63 (-14)	323±31 (-27)	328±56 (-25)	0.38 (-12)	0.38 (-4)
	T2	787±265 (-22)	884±53 (-12)	296±115 (-33)	332±52 (-25)	0.38 (-12)	0.38 (-12)
	T3	1003±135 (-1)	952±31 (-6)	413±77 (-6)	378±20 (-14)	0.41 (-3)	0.40 (-4)
	T4	1062±159 (+5)	1016±28 (+1)	462±101 (+5)	427±23 (-3)	0.44 (0)	0.42 (-2)
	T5	1071±160 (+6)	1058±21 (+5)	471±121 (+7)	452±21 (+3)	0.44 (0)	0.43 (-1)
Downstream	Baseline	826	826	192	192	0.23	0.23
	T1	579±63 (-30)	590±55 (-29)	102±13 (-47)	107±19 (-44)	0.18 (-5)	0.18 (-5)
	T2	557±183 (-32)	589±40 (-29)	89±43 (-54)	104±13 (-46)	0.16 (-7)	0.18 (-5)
	T3	721±108 (-13)	663±38 (-20)	141±34 (-27)	127±13 (-34)	0.20 (-3)	0.19 (-4)
	T4	743±128 (-10)	731±23 (-11)	150±46 (-22)	148±7 (-23)	0.20 (-3)	0.20 (-3)
	T5	785±101 (-5)	771±37 (-6)	173±36 (-10)	167±16 (-13)	0.22 (-1)	0.21 (-2)

805



806

**Table 6.** Contribution of climate and LU to the streamflow for different time periods

Region	Streamflow	P1 (1971-1980)	P2 (1981-1990)	P3 (1991-2000)	P4 (2001-2005)
Upstream	$Q_{\text{int}} (\text{m}^3\text{s}^{-1})$	775	772	859	823
	$Q_{\text{clim}} (\text{m}^3\text{s}^{-1})$	760	741	824	777
	$Q_{\text{clim}} (\%)$	98	96	96	94
	$Q_{\text{LU}} (\text{m}^3\text{s}^{-1})$	15	31	35	46
	$Q_{\text{LU}} (\%)$	2	4	4	6
Midstream	$Q_{\text{int}} (\text{m}^3\text{s}^{-1})$	1130	1183	1266	1195
	$Q_{\text{clim}} (\text{m}^3\text{s}^{-1})$	1108	1110	1182	1107
	$Q_{\text{clim}} (\%)$	98	94	93	93
	$Q_{\text{LU}} (\text{m}^3\text{s}^{-1})$	22	73	84	88
	$Q_{\text{LU}} (\%)$	2	6	7	7
Downstream	$Q_{\text{int}} (\text{m}^3\text{s}^{-1})$	123	103	85	78
	$Q_{\text{clim}} (\text{m}^3\text{s}^{-1})$	122	103	85	77
	$Q_{\text{clim}} (\%)$	100	100	99	98
	$Q_{\text{LU}} (\text{m}^3\text{s}^{-1})$	1	0	1	1
	$Q_{\text{LU}} (\%)$	0	0	1	2

807

**Table 7.** Contribution of LU and climate to streamflow during T1 (2010-2020) time slice under RCP 4.5 and RCP 8.5 emission scenarios

Streamflow	Upstream		Midstream		Downstream	
	RCP 4.5	RCP8.5	RCP 4.5	RCP8.5	RCP 4.5	RCP8.5
$Q_{\text{int}} (\text{m}^3\text{s}^{-1})$	800±72	789±28	1008±110	971±138	52±5	56±11
$Q_{\text{clim}} (\text{m}^3\text{s}^{-1})$	713±62	703±23	938±132	903±123	51±5	55±11
$Q_{\text{clim}} (\%)$	89	89	93	93	98	98
$Q_{\text{LU}} (\text{m}^3\text{s}^{-1})$	87±10	86±5	70±23	68±16	1±0	1±0
$Q_{\text{LU}} (\%)$	11	11	7	7	2	2

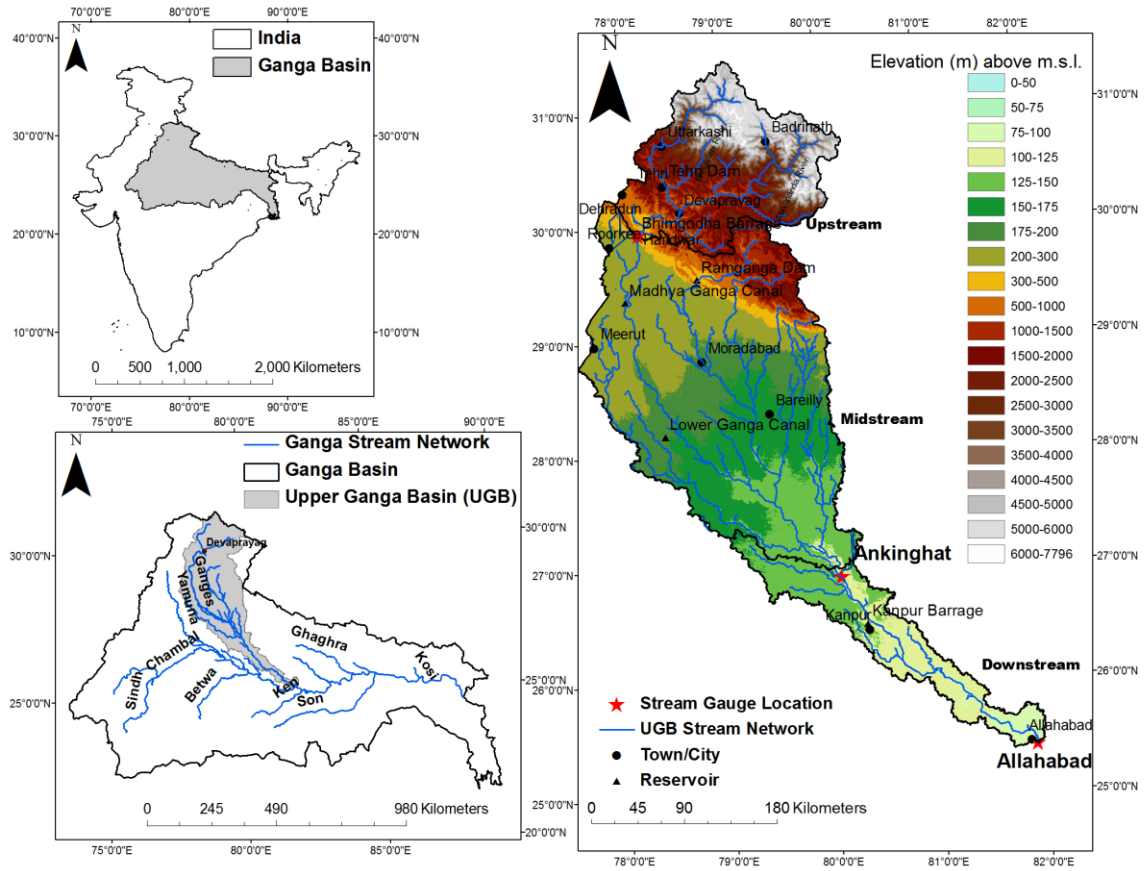


**Figure 1.** Location map and details of the UGB

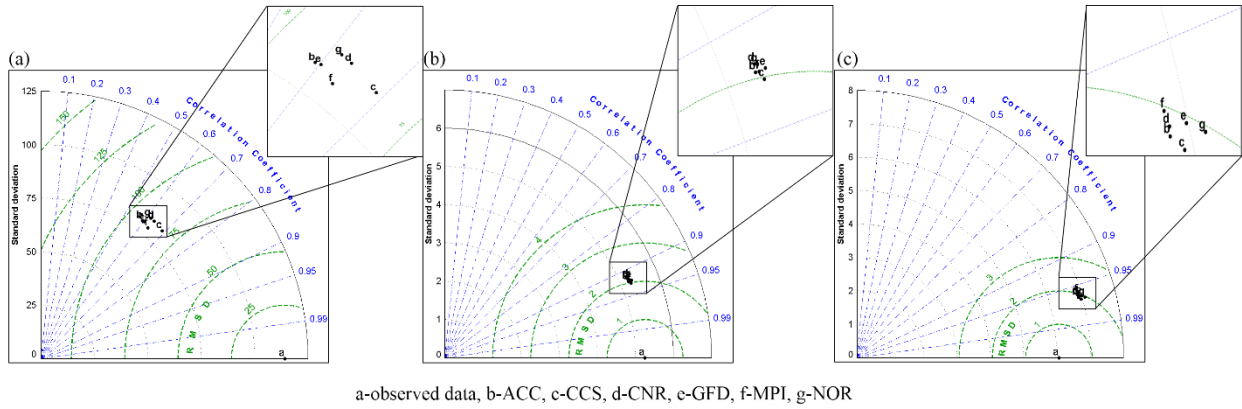


**Figure 2.** Taylor diagram for (a) Rainfall (mm) (b)  $T_{\max}$  (°C) and (c)  $T_{\min}$  (°C) for upstream region

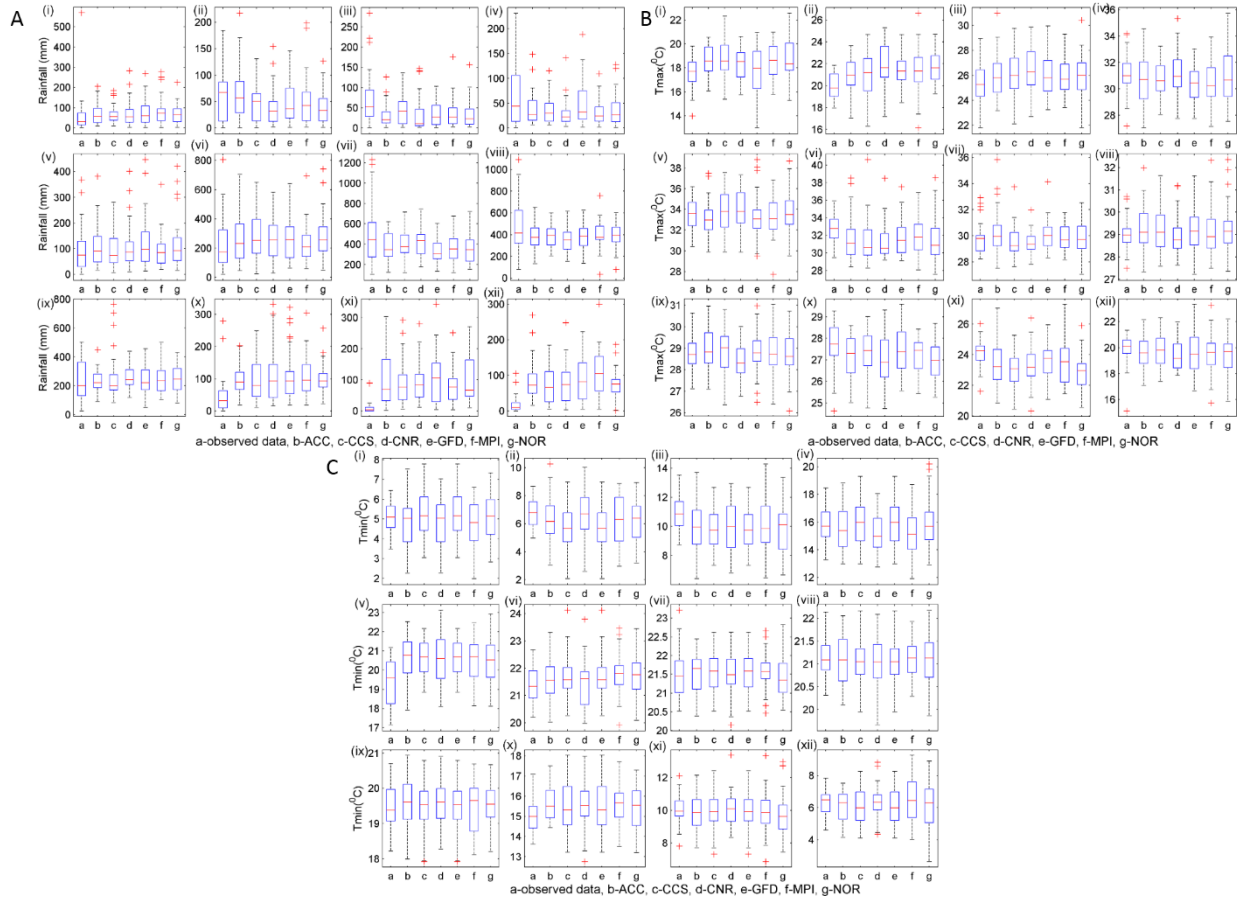


**Figure 3.** GCMs climatology compared with observed climatology for monthly (A) rainfall, (B) maximum temperature and (C) minimum temperature from 1971-2005 (represented from January-December as i-xii)

823

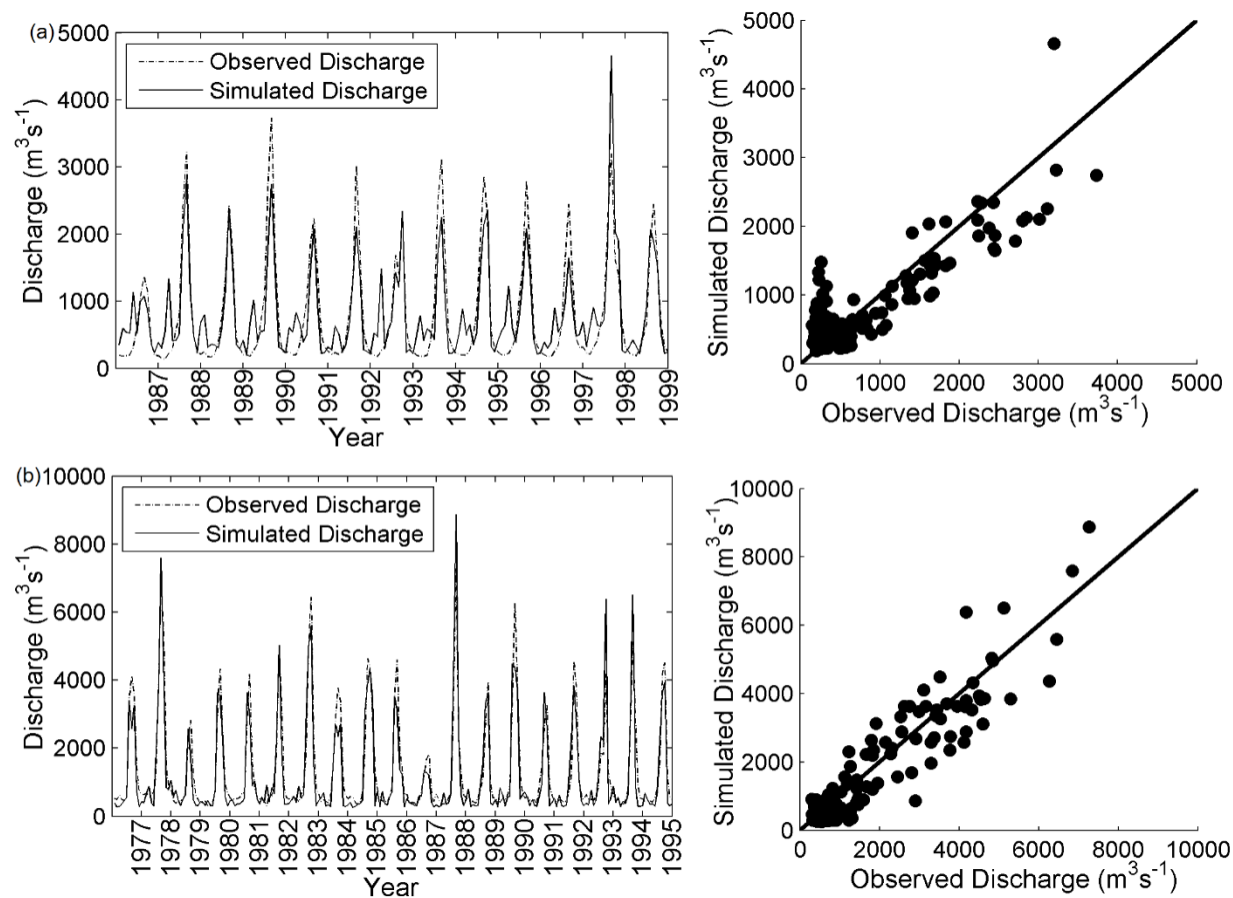


**Figure 4.** Calibration results of (a) Upstream and (b) Midstream region

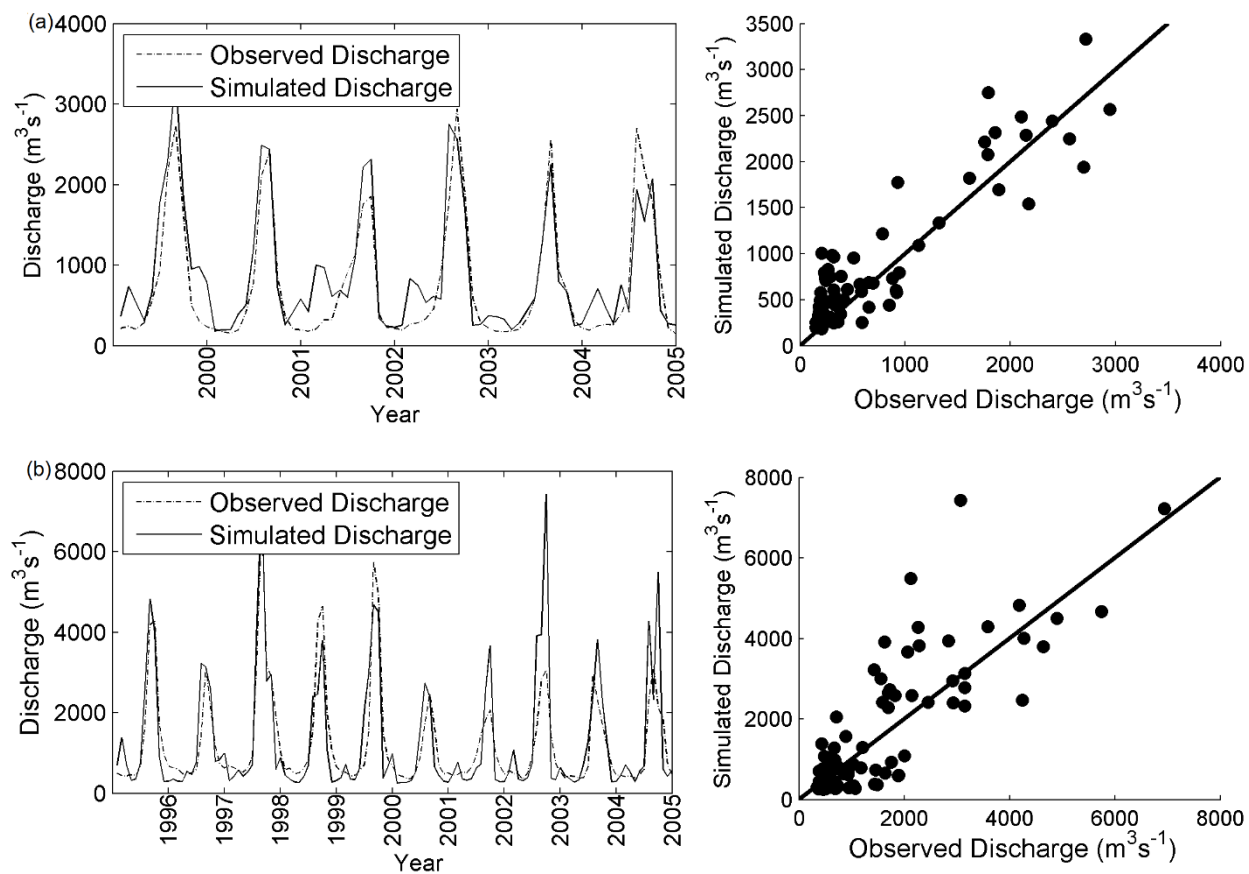


**Figure 5.** Validation results of (a) Upstream and (b) Midstream region

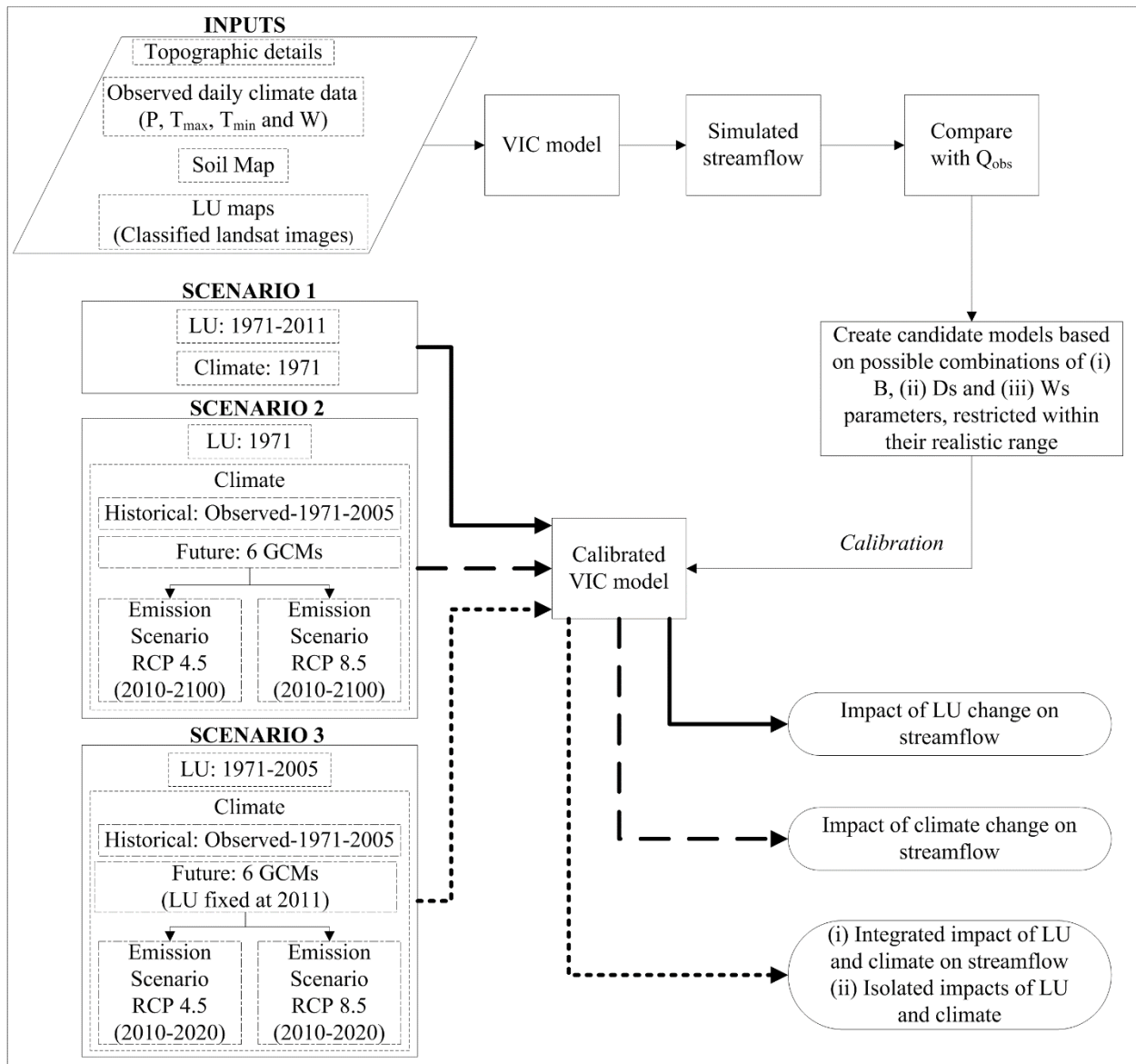


**Figure 6.** Overview of the work



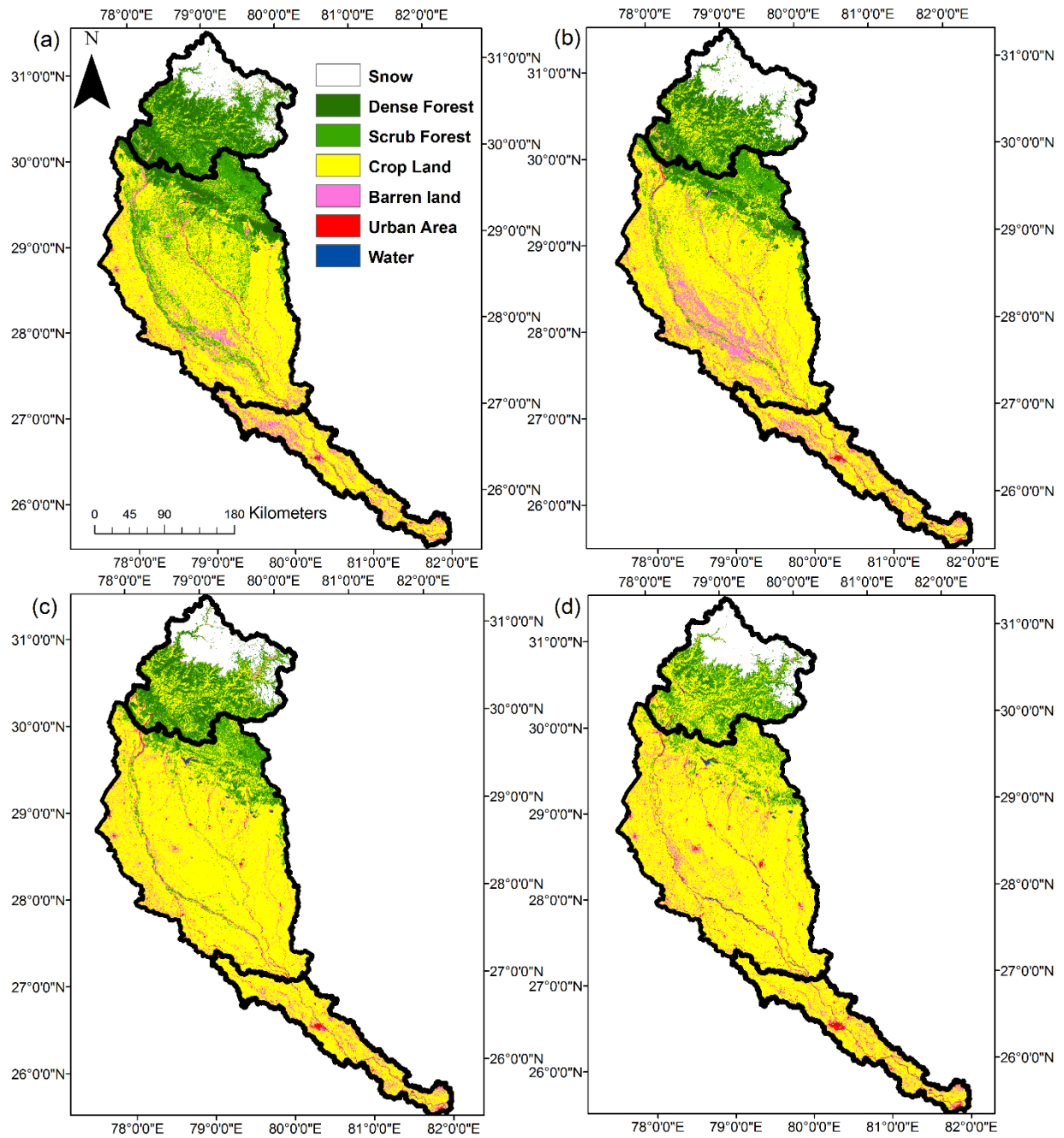


**Figure 7.** LU maps for (a) 1973, (b) 1980, (c) 2000 and (d) 2011

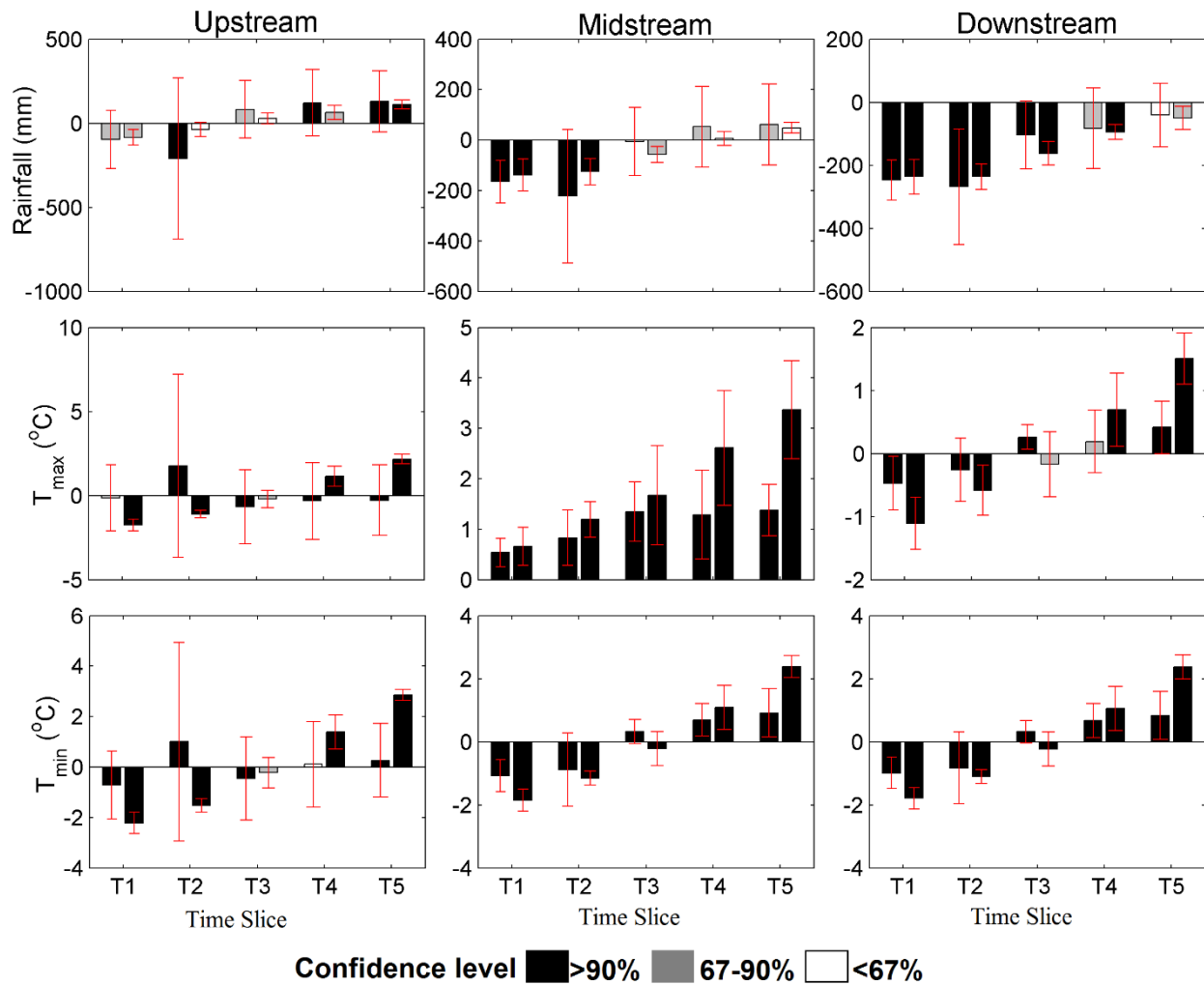


**Figure 8.** Change in the ensemble mean of rainfall (top panel),  $T_{\max}$  (center panel) and  $T_{\min}$  (bottom panel) from the baseline period for RCP 4.5 (first bar of a time slice) and RCP 8.5 scenarios (second bar of a time slice) at each time slice (T1: 2010-2020; T2: 2021-2040; T3: 2041-2060; T4: 2061-2080 and T5: 2081-2100)

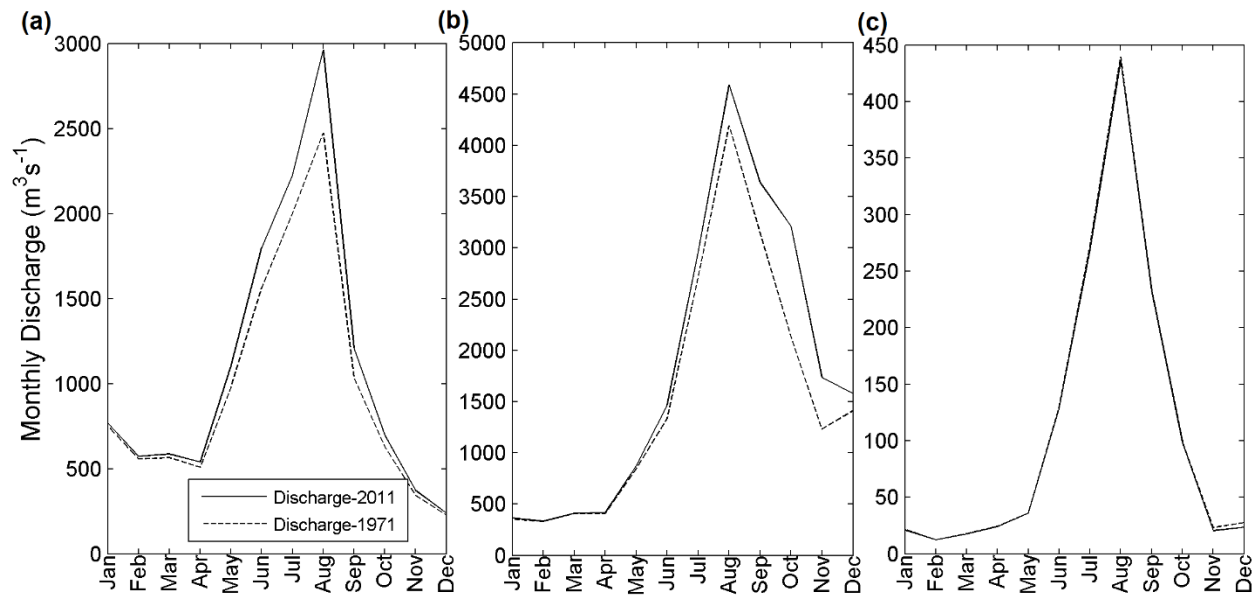


**Figure 9.** Simulation results for year 1971 and 2011 for (a) upstream, (b) midstream and (c) downstream region

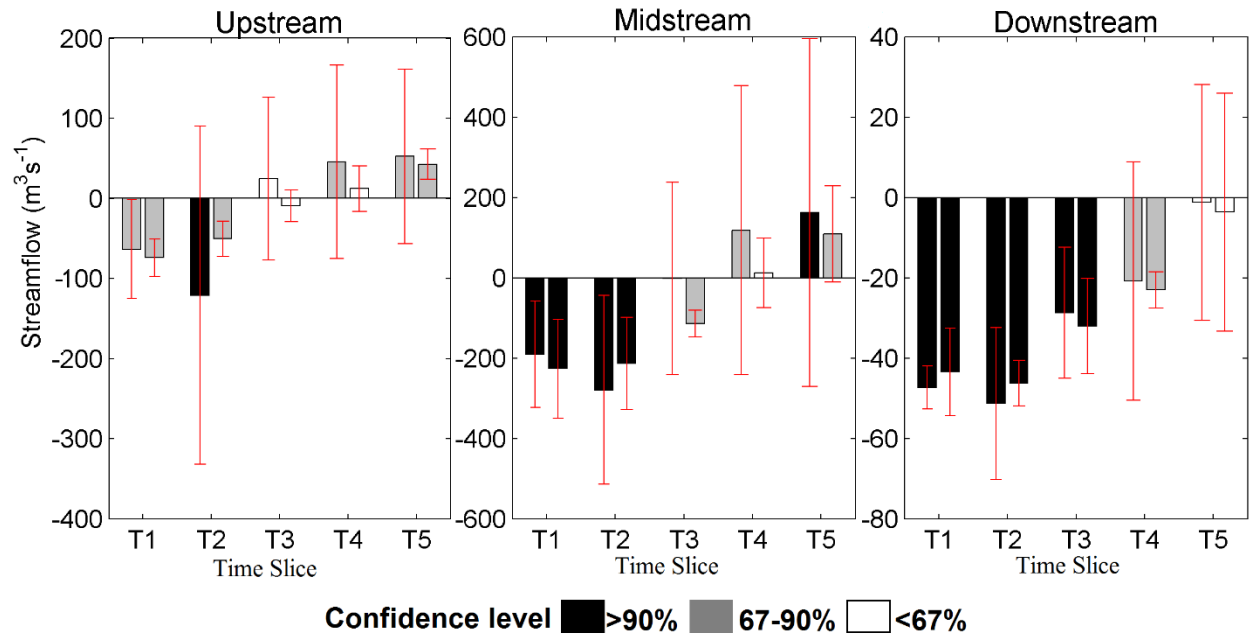


**Figure 10.** Change in ensemble mean of  $Q_{\text{clim}}$  from the baseline period for RCR 4.5 (first bar of every time slice of all the plots) and RCP 8.5 (second bar of every time slice of all the plots) scenarios at each time slice (T1: 2010-2020; T2: 2021-2040; T3: 2041-2060; T4: 2061-2080 and T5: 2081-2100)